Water evaporation reduction by the agrivoltaic systems development

Article *in* Solar Energy · October 2022

DOI: 10.1016/j.solener.2022.10.022

6 authors, including:

Altyeb Ali Abaker Omer
University of Science and Technology of China
18 PUBLICATIONS **55** CITATIONS
SEE PROFILE

Ming Li
University of Science and Technology of China
8 PUBLICATIONS **48** CITATIONS
SEE PROFILE

Samia Osman
University of Science and Technology of China
3 PUBLICATIONS **3** CITATIONS
SEE PROFILE

Jianan Zheng
University of Science and Technology of China
5 PUBLICATIONS **14** CITATIONS
SEE PROFILE

Solar Energy 247 (2022) 13–23

Contents lists available at ScienceDirect

Solar Energy

journal homepage: www.elsevier.com/locate/solener

Water evaporation reduction by the agrivoltaic systems development

Altyeb Ali Abaker Omer, Wen Liu *, Ming Li *, Jianan Zheng, Fangxin Zhang, Xinyu Zhang, Samia Osman Hamid Mohammed, Liulu Fan, Zhipeng Liu, Fangcai Chen, Yuxuan Chen, Jan Ingenhoff

Department of Optics and Optical Engineering, School of Physics, University of Science and Technology of China, Hefei 230026, China

ARTICLE INFO

Keywords:
Agrivoltaic systems development
Spectral separation
Even-lighting
Soil water evaporation
Water Saving

ABSTRACT

The triple benefits of the AgriVoltaic Systems Development (AVSD) have been well demonstrated, not only for the PV electricity generation but also for reduced water evaporation, enhancing further the benefits of simultaneously crop growth on the same land area. However, the reduction rate of the water evaporation of AVSD has not been investigated in a quantitative way. Therefore, this study conducted experiments to measure water evaporation reduction under the Concentrated-lighting Agrivoltaic System (CAS) and the Even-lighting Agrivoltaic System (EAS). Evaporation containers and pans were placed in the bare soil (CK) under the CAS and the EAS. Our results showed a significant reduction in water evaporation under CAS and EAS. Cumulative soil surface evaporation of CK, CAS, and EAS for 45 days was 80.53 mm, 63.38 mm, and 54.14 mm. The cumulative water evaporation from soil and pan surfaces decreased by 21 % and 14 % (under CAS), 33 %, and 19 % (under EAS), respectively. The slope $\beta_1 \neq 0$ of simple linear regression showed a significant positive relationship between evaporation time and cumulative water evaporation. The correlation coefficient in all treatments was more than 0.91, suggesting a robust linear relationship. The feasibility of AVSD could significantly reduce irrigation water, enhance crop growth, and generate electricity simultaneously on the same agricultural land.

1. Introduction

Water scarcity is an increasingly critical issue in many parts of the world (AbdAllah 2019, El-Ghannam et al 2021, Greve et al 2018, Li et al 2021a, Morsy et al 2021, Shalaby et al 2021). It is expected to worsen with population growth and climate change (AbdAllah et al 2019, Hunt et al 2020). By 2050 (2012), the water shortage problem may affect more than 40 % of the world's population, particularly in arid and semi-arid areas (Abdallah et al 2021, Li et al 2021a). Evaporation is a constant and essential process in the water cycle (Abdallah et al 2021, Condon et al 2020, Mueller et al 2013, Zhao & Gao 2019). Temperature, wind speed, relative humidity, and solar radiation are the critical climatic components influencing water surface evaporation (Meziani et al 2020). Evaporation increases when the humidity drops, the air becomes warmer, or the wind strengthens (Nguyen et al 2020). However, not all of these factors contribute equally to water evaporation. A vapor pressure deficit is the main factor for increasing evaporation (Meziani et al 2020).

Various approaches were conducted to reduce water evaporation (Kasirajan & Ngouajio 2012, Knowles et al 2012, Lemon 1956, Xie et al 2006). The worries about water resources have prompted the development of techniques for reducing soil evaporation (Waheeb Youssef & Khodzinskaya 2019). Among these techniques, mulches are applied worldwide to the soil surface to reduce water evaporation. Typical mulches applied are gravel mulches (Adams 1966, Awodoyin et al 2010, Yuan et al 2009), organic mulches (Liao et al 2021, Zribi et al 2015), synthetic mulches (Awan 2009, Kasirajan & Ngouajio 2012, Khorsandi 2011, Wu et al 2017, Zribi et al 2015), and shading material mulches (Alvarez et al 2006, Tesfuhuney et al 2015). Mulching has numerous advantages for agricultural land. However, using many organic and synthetic mulches on farmlands restricts air, water, and light from reaching the soil. In addition, the synthetic mulch typically needs to be replaced every time. This, in turn, results in excessive heat, acidity levels, and bacteria. Therefore, it often has more disadvantages than advantages (Loz November 17, 2020, Nyamoti 16/6/2020). To protect agricultural land from such risks of mulches applied on farmlands, solve the harmful effects of climate change, and find solutions to save water on farming lands. Some researchers have used agrivoltaic systems to provide multi-benefits across food, energy, and water connections (Barron-Gafford et al 2019, Elamri et al 2018, McKuin et al 2021, Riaz et al 2021).

* Corresponding authors.
E-mail addresses: wenliu@ustc.edu.cn (W. Liu), mingxin@ustc.edu.cn (M. Li).

https://doi.org/10.1016/j.solener.2022.10.022
Received 24 January 2022; Received in revised form 10 August 2022; Accepted 8 October 2022

Nomenclature

E_{ms}	Soil surface evaporation (kg/day)
E_{mp}	Pan surface evaporation (kg/day)
E_{ss}	Soil surface evaporation (mm/day)
E_{sp}	Pan surface evaporation (mm/day)
A_{soil} :	The area of the soil surface (cm^2)
A_{pan}	The area of the pan surface(cm^2)
M_s	The mass of dry soil (kg)
M_{ds}	The mass of the air-dried soil (kg)
θ_{ds}	The water content of the air-dried soil (m^3/m^3)
θ_v	The volumetric water content (kg)
θ_g	The gravimetric water content (kg)
ρ_{soil}	The density of the air-dry soil (g/m^3)
ρ_{water}	The density of water (g/m^3)
m_{wet}	The weight of wet soil (kg)
m_{dry}	The weight of dry soil (kg)
M_{aw}	The absorbed water (kg)
M_1	The initial mass of the soil (kg)
E_{msi}	The surfaces evaporation on an i^{th} day ($i = 1, 2, \ldots\ldots, 45$)
M_i	The masses of the soil water on an i^{th} day ($i = 1, 2, \ldots\ldots, 45$)
θ_i	The soil water content on an i^{th} day ($i = 1, 2, \ldots\ldots, 45$)
β_0	The regression line's y-intercept
β_1	The regression line's slope
ε	The error term
$\widehat{y}$	The anticipated y value
b_0	The line's y-intercept
b_1	The line's slope

Abbreviation

AVSD	AgriVoltaic Systems Development
CAS	Concentrated-lighting Agrivoltaic System
EAS	Even-lighting Agrivoltaic System
CK	Bare soil (control treatment)
PV	Photovoltaic
TAS	Traditional Agrivoltaic Systems
R	Correlation coefficient
R^2	Coefficient of determination
SPSS	Statistical Package for the Social Sciences
ANOVA	Analysis of variance
d	The unit of the evaporation time (day)
S1, S2, S3, and S4	Supplementary data

The first agrivoltaic system was proposed in the 1980s (Goetzberger & Zastrow 1982). Today, the agrivoltaic system is being implemented in many countries to simultaneously combine renewable energy with agricultural production on the same land (Gorjian et al 2022, Jones et al 2022, Lu et al 2022, Neupane Bhandari et al 2021, Schindele et al 2020, Weselek et al 2021, Xue 2017). Currently, there are two Traditional Agrivoltaic Systems (TAS) solutions. The first is achieved by putting mosaic or strip photovoltaic panels in the agricultural field (Obergfell et al 2013). They enable part of sunlight to reach the ground. Still, most of the sunlight is blocked by the solar panels, and the plants under the solar panels can only stay in the scattering sunlight, which typically is about 15 ~ 20 % of total solar energy. Another TAS is the application on greenhouse roofs. Numerous studies have documented the integration of photovoltaic greenhouses (Allardyce et al 2017, Cossu et al 2014, Hassanien et al 2018, Kumar et al 2022, Yano et al 2009, Yano et al 2010) and thin-film greenhouse roofs (Sonneveld et al 2010a, Sonneveld et al 2010b). The PV panels or thin-film solar panels cover the greenhouse roof just partially. Again, the shade of PV panels or thin-film solar panels affects plant growth. The amount of sunlight transferred through thin-film solar panels may not be enough to ensure efficient plant photosynthesis.

Plants require sufficient light for photosynthesis; red and blue lights are the most important for plant photosynthesis (Kasahara et al 2004). Far-red light also affects the morphology and growth of plants in different forms at various stages of plant growth (Hwang et al 2020). The PV modules above farmland also have a shading effect and, in the same way, decrease crop yield and quality. Homma et al (2016) found that rice yield was reduced under the TAS due to shade increase. Tomatoes grown under agrivoltaic greenhouses have lower masses and prolonged ripening times compared to conventional greenhouse vegetables (Marrou et al 2013). Moreover, the experimental results of shade-tolerant crops such as lettuce also showed a yield reduction of 20 ~ 40 % (Marrou et al 2013, Valle et al 2017). However, in drylands or under severe water stress, the TAS helps avoid drought stress and maintain higher soil moisture, improving plant growth (Barron-Gafford et al 2019, Hassanpour Adeh et al 2018). Based on the above research, the TAS significantly increases crop yield in environments that are not favorable for plant growth, like excessive sunlight, high temperatures, droughts, and water shortages. Nevertheless, it also leads to evident reductions in crop yield and quality where the climate is suitable for growth. These researches indicate that TAS cannot simultaneously resolve the conflict between crop photosynthesis and PV power generation.

We proposed two solutions to solve the challenge of simultaneously allowing crop photosynthesis and PV electricity generation on the same farmland. The first solution is CAS (Liu et al 2018) based on spectral separation, which selectively transmits red, blue, and far-red light from the sunlight to reach the plants for photosynthesis. The rest of the sunlight is concentrated and reflected on PV panels for electricity generation. The key to the solution is to design a multi-passband filter film enabling this sunlight separation under a low cost. The multiplication co-extrusion process, which is capable of economic and continuous production, has been adopted to prepare alternately superimposed multilayer films (Andrews et al 2012, Singer et al 2008, Weber et al 2000). The other solution is EAS (Zheng et al 2021). The core idea is to improve the TAS structure design by placing grooved glass plates between two conventional PV panels. They allow for transmission and distribute sunlight evenly with a uniform illumination providing sufficient light intensity for plant photosynthesis. The top of the PV panels between the grooved glass plates are hit by the sunlight in a conventional way to generate electricity. Whether CAS or EAS, the soil and water surfaces under the systems are exposed indirectly by the sunlight; therefore, the soil moisture content is higher than any soil surface exposed directly by the sunlight. Our previous studies (Liu et al 2018, Zheng et al 2021) confirm that using AVSD the crops can grow well and the PV panels can generate electricity efficiently and simultaneously on the same land. Furthermore, water evaporation was reduced and enhanced crop growth. However, the amount of reduced water evaporation under the AVSD has not been quantified or calculated yet. Therefore, this study's main objectives are (1) calculating the reduction of cumulative water evaporation under the AVSD. (2) investigating the mechanism of evaporation reduction under the AVSD.

2. Experimental materials and methods

2.1. Experimental site

Experiments were conducted at Fuyang City, Anhui Province in China, at latitude 32°58 N, longitude 115°55 E, and 4 m above sea level. Fuyang city is located on the southwestern edge of the Huanghuai Plain

Table 1
Soil's basic physical and chemical parameters in the experiment region.

Soil Properties	Units	Value
pH		8.21
Organic matter	g kg^{-1}	4.37
Total nitrogen	%	0.034
Hydrolyzable nitrogen	mg kg^{-1}	28.4
Available phosphorus	mg kg^{-1}	2.3
Quick-acting potassium	mg kg^{-1}	163
Bulk density (ρbulk)	g cm^{-3}	0.995
Porosity (ε)	%	0.617
0 to 2 μm (Clay)	%	8.49
2 to 50 μm (Powder)	%	79.79
50 to 2000 μm (Sand grain)	%	11.69

and in the northwest Anhui Province. A warm temperate semi-humid monsoon climate characterizes the region. The weather is mild, and the rainfall is moderate. The yearly average rainfall is 820–950 mm. The annual sunshine hours are 2200–2500 h, the frost-free period is 220–230 days, and the annual average relative humidity is 58.5 %.

2.2. Experimental materials

Air-dried loamy soil was used in the experiment. The physical properties and chemical properties of soil are shown in Table 1. Sichuan Huabiao Testing Technology Co. ltd. Chengdu, Sichuan 610016, China, conducted soil properties tests.

In this experiment, we used an evaporated container (white plastic buckets) with a temperature resistance of + 130 °C, a low-temperature resistance of −30 °C, and a weight of 406 g. It has a top diameter of 26.0 cm, a bottom diameter of 22.0 cm, and a height of 28.5 cm. It has nine holes at the bottom, each having a diameter of 1 cm.

In this experiment, we used Chinese standard pan evaporation (Model ADM7, made in China), a stainless-steel metal cylinder, and a bottom cover. The wall thickness was 5 mm, the diameter was 20 cm, and the depth was 11 cm (Khorsandi 2011, Liu & Kang 2007, Liu et al 2018).

For this experiment, we set up three weather stations. The first was conducted in CK, the second under CAS, and the third under EAS. Each day, micrometeorological data were collected (from 8:00 morning. to 8:00 morning the following day). Data loggers recorded the air temperature (°C), wind speed (m s^{-1}), relative humidity (%), and solar radiation (W m^{-2}) during testing time.

2.3. The agrivoltaic systems development (AVSD)

2.3.1. The Concentrated-lighting Agrivoltaic System (CAS)

The CAS solution was invented in 2015 to solve the PV blocking sunlight for plant photosynthesis. We used bent glass panels covered by low-cost multilayer interference films (Fig. 1b) to match the transmission of the red, blue, and far-red light spectrum for plant photosynthesis. The rest sunlight wavelengths reflect for generating electricity, as shown in Fig. 1a. Fig. 1 c and d show the agrivoltaic system application in Fuyang City. The purpose was to transmit blue, red, and far-red light at 450 nm ± 20 nm, 660 nm ± 20 nm, and 735 ± 30 nm, respectively, for plant growth. And reflectivity of all other wavelengths to expected to be very high (~90 %) (Li et al 2021c). The CAS system's basic idea, design, and work principle are shown and discussed in our previous studies (Liu et al 2017, Zhang et al 2018). The cultivation and observation of plants, such as lettuce, cabbage, cucumber, and other plants, were better under the polymer interference multilayer film than the non-film control plants concerning yield and quality photosynthetic index (Liu et al 2018). Furthermore, multilayer films covered with curve glass

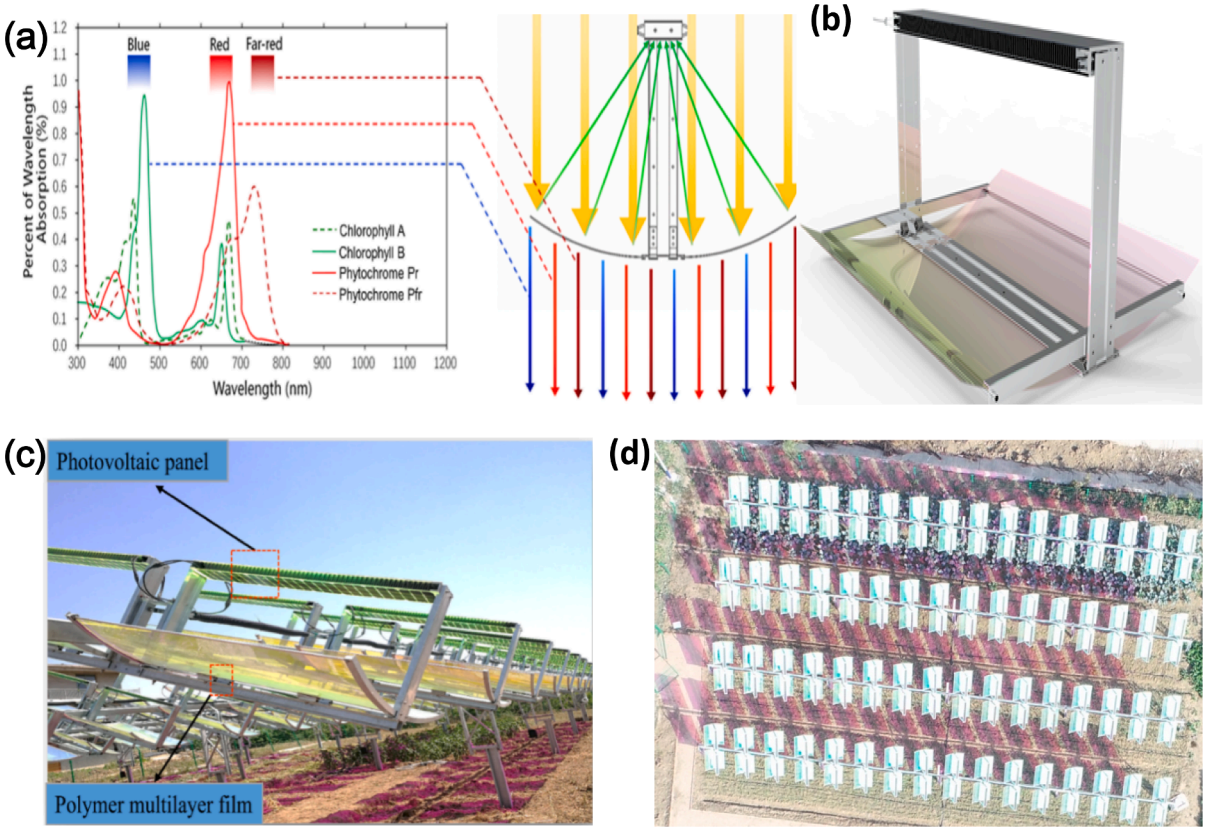

Fig. 1. The structure design of The Concentrated-lighting Agrivoltaic System (CAS) (a) Spectral required for plant photosynthesis and solar power generation (b) Polymer multilayer film attached to curved glass panels (c) the side section and (d) the top section of CAS applied in the agricultural field in Fu yang City, Anhui province. China.

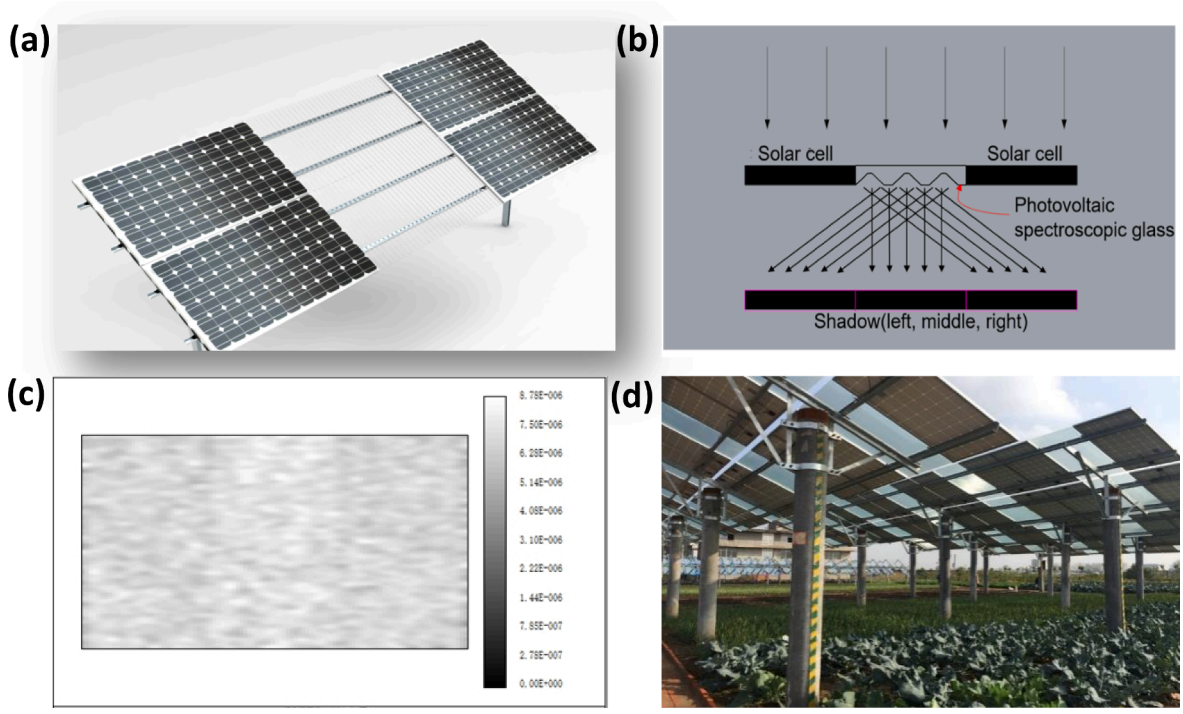

Fig. 2. The structural design of the Even-lighting Agrivoltaic System (a) shows a grooved glass plate inserted between two conventional solar photovoltaic panels to achieve beam splitting (b) Light path of the optical simulation (c) The illuminance simulation results of the glass plate and (d) the Even-lighting Agrivoltaic System applied in the agricultural field in Fu yang City, Anhui province. China.

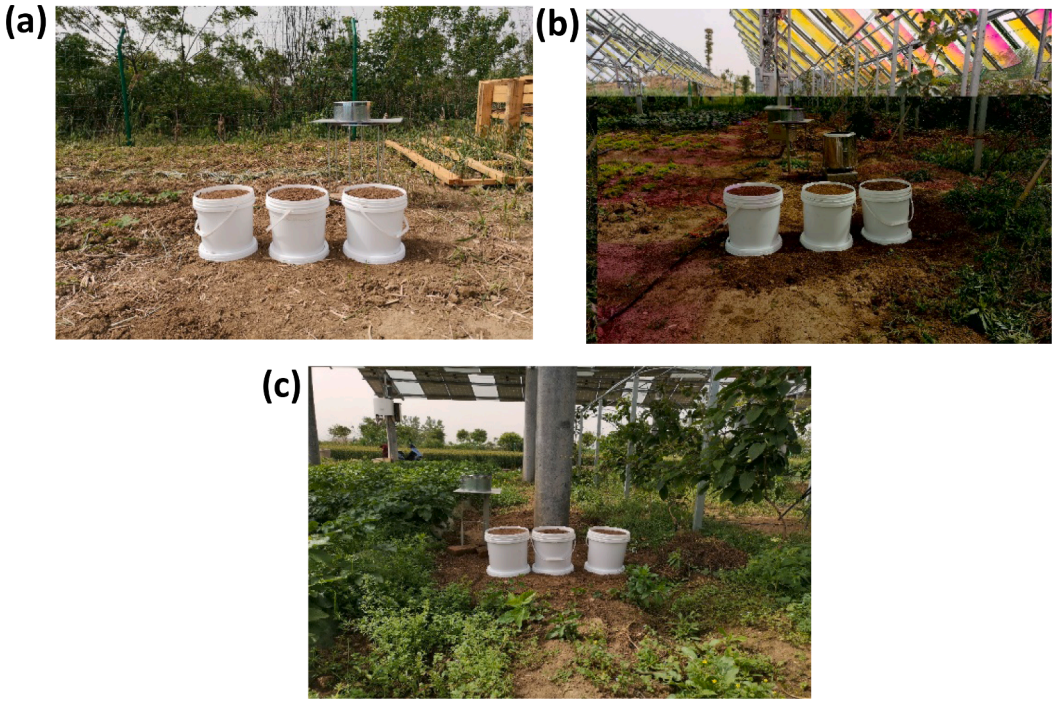

Fig. 3. The design of three experiment treatments of evaporation containers and pans evaporation placed (a) in bare soil, (b) under a Concentrated-lighting Agrivoltaic System, and (c) Even-lighting Agrivoltaic System.

showed significantly reduced water evaporation(Ali Abaker Omer et al 2022).

2.3.2. The Even-lighting Agrivoltaic System (EAS)

The EAS solution solves the problem of the non-uniform intensity distribution under the existing TAS. It can satisfy shade-requiring crops' growth by inserting grooved glass plates between conventional PV panels, as shown in Fig. 2a. Fig. 2b, shown in SolidWorks2017, was used to build a model for the grooved glass plate. ZEMAX software was used to do the optical simulation to test and verify the accuracy of the groove glass plate. The design quality is determined such that a detector beneath the EAS system receives uniform illumination. A simulation of

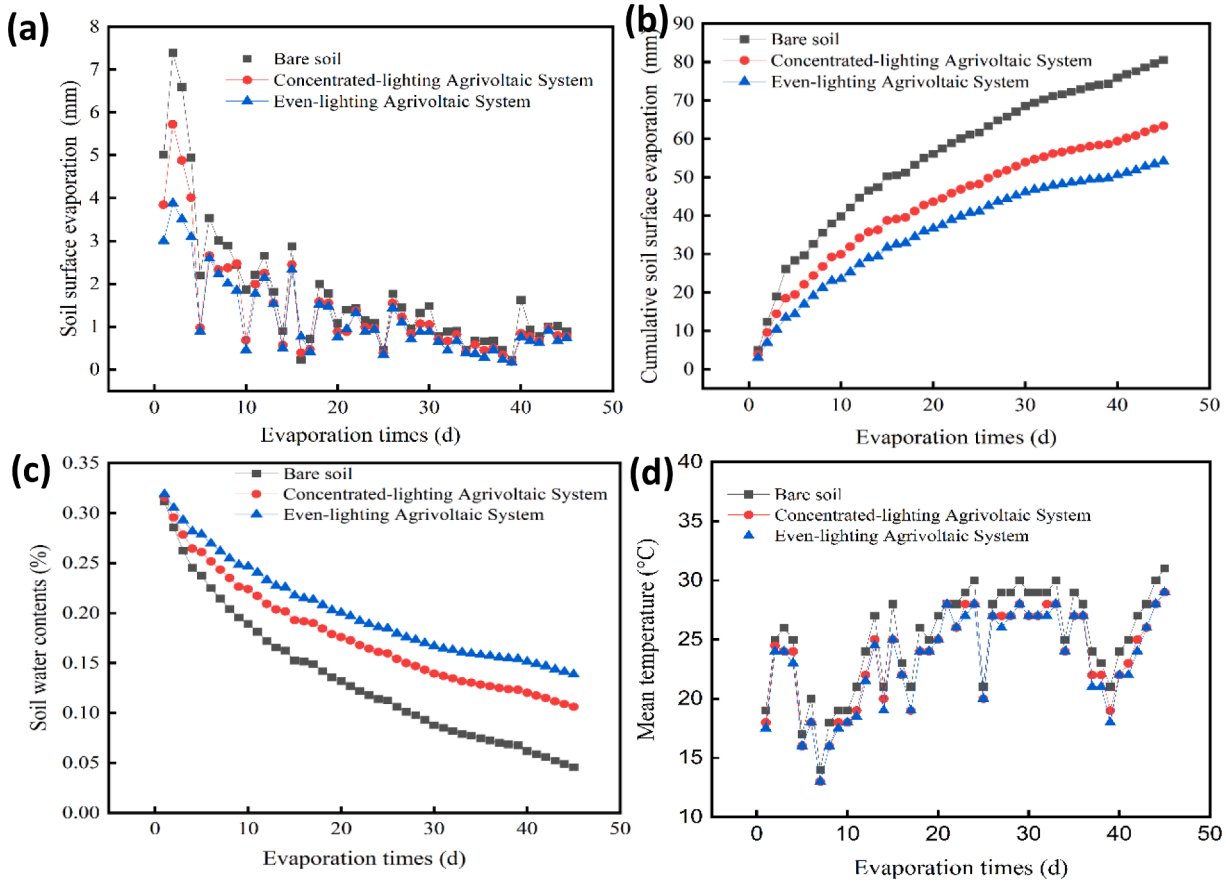

Fig. 4. The effect of the three experiments on the evaporation of water from the soil surface (a) daily soil surface evaporation (mm), (b) cumulative soil surface evaporation (mm), and (c) soil water content (%). (d) mean temperature (∘C).

the optical path is shown in Fig. 2c. The rectangular light source can radiate uniform parallel light; SolidWorks2017 modeled the grooved glass plates, separating the light into three parts as expected. An illuminance detector behind the glass received uniform pixels. We obtained illuminance simulation results for the glass plate, as shown in Fig. 2c. the sensor received 0.32 W of optical power. Still, only one-third of the optical power was irradiated on the groove glass plate. We calculated that the groove glass plates have a transmittance of 96.6 %. We then replaced the rectangular detector with three smaller rectangular sensors on the shadow region's left, middle, and right sides; each received 0.104 W, 0.114 W, and 0.103 W of optical power. In our opinion, the groove glass plate achieves uniform light-splitting with slight variations. The vegetables/crops planted beneath the system showed significant growth and yield improvement. Our previous studies show the basic idea of the system, design, and work principle (Zheng et al 2021, Zheng et al 2019).

2.4. Experimental design and procedures

In this experiment, we used loam soil from the 0 to15 cm layer of an agricultural field, the most common type of soil found in the region. We dried the soil for 78 h and mixed it carefully to achieve uniform moisture distribution. In evaporation containers, screens were placed to prevent soil particles from leaking. The air-dried soil was packed into the evaporation containers to a depth of 25 cm. The soil was filled in the evaporation containers, and the containers were placed at a 10 cm water depth. For 48 h, water was transported from the bottom holes to the soil surface of containers via capillary forces. We removed the evaporation containers from the water tank to discharge residual water for 24 h through the bottom holes. The soil containers were covered with plastic sheets to prevent soil evaporation. Afterward, the evaporation containers were weighed. Fig. 3 shows the design of the three experimental treatments. The evaporation containers and pans were placed in CK, under CAS, and EAS. Three replicates were used in each experimental treatment.

In comparison, an experiment on evaporation was conducted in natural settings at the initial soil water content of the field capacity. During rain periods, the evaporation containers were covered with plastic sheets. We used an electronic scale of 30 ± 1 kg to weigh the evaporation containers and pans daily at 8:00 a.m. the experiments lasted 45 days during the summer season from May 8th to June 25th, 2021. Using data loggers, weather stations recorded the daily temperature, relative humidity, wind speed, and solar radiation.

2.5. Experimental data analysis

The soil surface evaporation volumes (E_{ms}) were calculated based on the weight changes of the evaporation containers. In addition, the pan surface evaporation volume recorded (E_{mp}). In the following equations, soil surface evaporation E_{ms} (kg/day) and pan surface evaporation E_{mp} (kg/day) are converted into soil surface evaporation E_{ss} (mm/day) and pan surface evaporation E_{sp} (mm/day) (Yuan et al 2009):

$$E_{ss} = E_{ms} \times 1000\left(cm^3 kg^{-1}\right) \times \frac{10(mm^1 cm^{-1})}{A_{soil}} \quad (1)$$

$$E_{sp} = E_{mp} \times 1000\left(cm^3 kg^{-1}\right) \times \frac{10(mm^1 cm^{-1})}{A_{pan}} \quad (2)$$

where A_{soil} : the area of the soil surface (cm^2), and A_{pan}: the area of the pan surface(cm^2).

To calculate the dry soil mass, use the following formula M_s(Yuan et

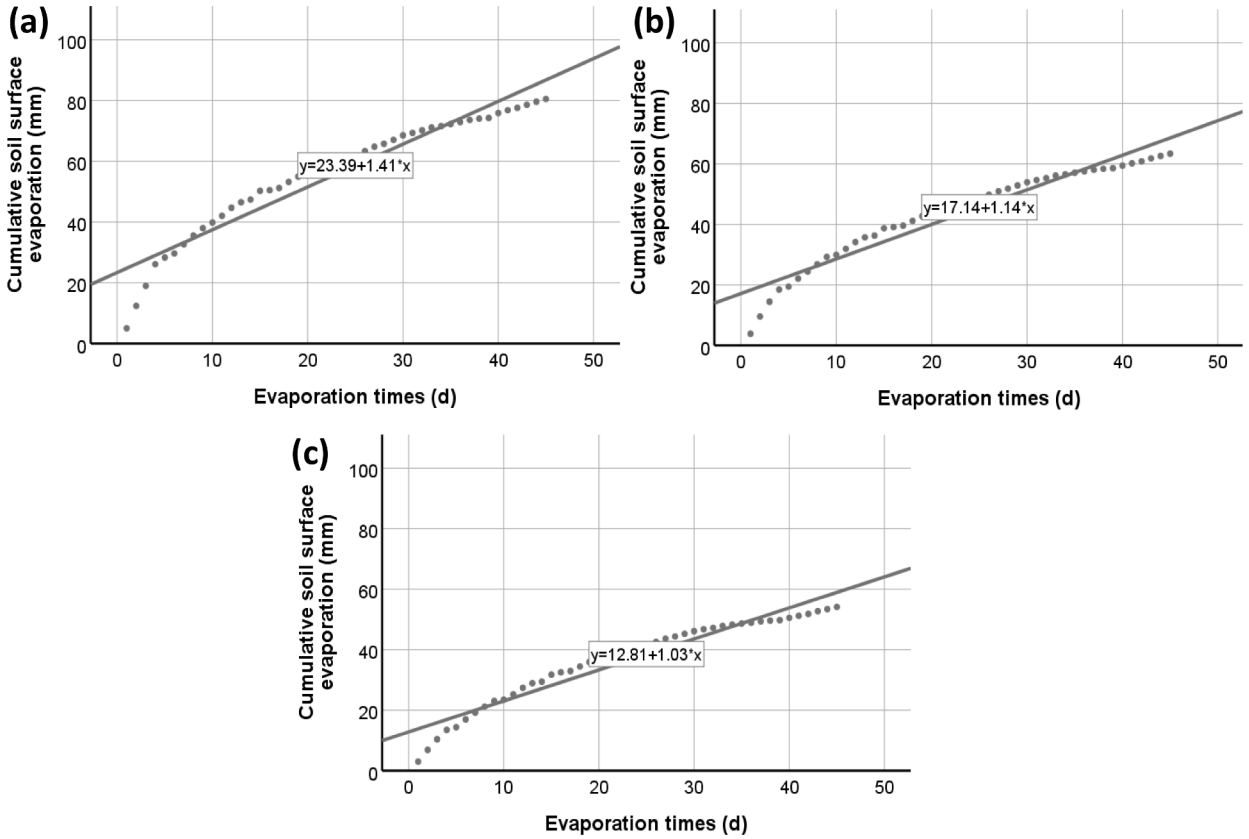

Fig. 5. Cumulative soil surface evaporation and evaporation time under three treatments basis on the fitting equation (a) bare soil, (b) under Concentrated-lighting Agrivoltaic System, and (c) Even-lighting Agrivoltaic System.

al 2009):

$$M_s = \frac{M_{ds}}{1+\theta_{ds}} \tag{3}$$

where *the* θ_{ds} : water content of the air-dried soil (m^3m^{-3}), and the M_{ds}: mass of air-dried soil (kg).

The volumetric water content (θ_v) of soil is the amount of liquid water per unit volume. By dividing mass by density (ρ), volume is calculated as follows (By Jim Bilskie):

$$\theta_v = \frac{\theta_g \rho_{soil}}{\rho_{water}} \tag{4}$$

where θ_g: Gravimetric water content (kg), ρ_{soil}: the density of the air-dry soil (g cm^{-3}), ρ_{water}: the density of water, which is close to 1 g cm^{-3}. The mass of water per mass of dry soil is known as gravimetric water content (θ_g) (By Jim Bilskie). It is the mass of water per mass of dry soil. The value of (θ_g) is obtained by subtracting the weight of dry soil (m_{dry}) from the weight of wet soil (m_{wet}), and then dividing by the weight of dry soil.

$$\theta_g = \frac{m_{wet} - m_{dry}}{m_{dry}} \tag{5}$$

On the first day (M_1), the initial masses of the soil water are calculated by the following equation: (Yuan et al 2009):

$$M_1 = M_{aw} + M_s \times \theta_{ds} \tag{6}$$

where M_{aw} Is the absorbed water (kg) (the absorbed water is the weight of change of the evaporation containers before and after being placed in the water tank), M_s Is the dry soil mass in (kg), and θ_{ds} Is the air-dried soil water content in (m^3m^{-3}). The surface evaporation on an i th day is given as E_{msi} ($i = 1, 2, \ldots\ldots\ldots, 45$), while the masses of the soil water on an i th day (M_i) are:

$$M_i = M_{i-1} - E_{msi-1} (i = 2, 3, \cdots\cdots\cdots, 45) \tag{7}$$

On an i th day, the soil water content θ_i It is estimated as follows:

$$\theta_i = \frac{M_i}{M_s} (i = 1, 2, \cdots\cdots\cdots.., 45)^s \tag{8}$$

2.6. Statistical analysis: We applied a linear regression model:

$$y = \beta_0 + \beta_1 x + \varepsilon \tag{9}$$

where β_0 is the regression line's y-intercept, β_1 is the regression line's slope, and ε is the error term. The population parameters are b_0 *and* b_1: the sample statistics used to estimate β_0 *and* β_1 are b_0 *and* b_1.

$$\hat{y} = b_0 + b_1 x \tag{10}$$

where $\hat{y}$ Is the anticipated y value for a given × value, b_0 is the line's y-intercept, and b_1 is the line's slope.

The gradient (β_1) is tested for significance between the cumulative water evaporation and evaporation times. If the gradient of the line $\beta_1 \neq 0$, there is a relationship between cumulative water evaporation and evaporation times. Tests for significance of the slope coefficient of the regression model were using a level of $\alpha = 0.05$ (Loftus 2022). The SPSS25.0 program was used to estimate the linear regression equation, R^2 (coefficient of determination), R (correlation coefficient), and ANOVA test.

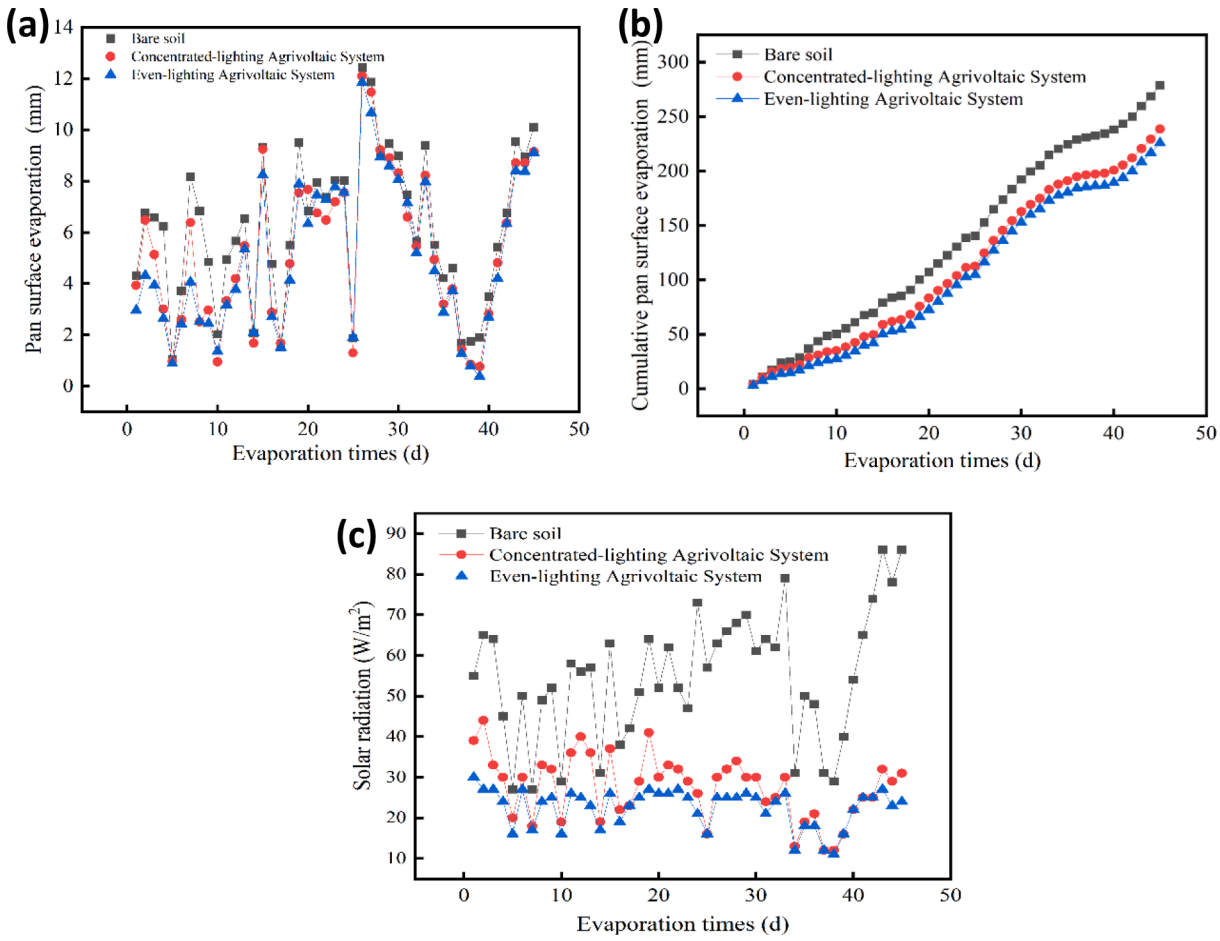

Fig. 6. The effect of the three experiments on the evaporation of water from the surface of the pan (a) daily water surface evaporation (mm), (b) cumulative pan surface evaporation (mm), and (c) solar radiation (W/m2).

Table 2
The output of the SPSS shows the model Summary[b] of the three treatments.

Mode	R	R^2	Adjusted R^2	Standard Error of the Estimate
The bare soil				
1	0.962a	0.925	0.923	5.32244
Concentrated-lighting Agrivoltaic System				
1	0.965a	0.932	0.930	4.11391
Even-lighting Agrivoltaic System				
1	0.967a	0.936	0.934	3.57019

a. Predictors: (Constant), Evaporation time (d), and b. Dependent Variable: Cumulative soil surface evaporation (mm).

Table 3
The output of the SPSS shows the analysis variance (ANOVA[a]) of the three treatments.

Mode		Sum of Squares	df	Mean Square	F	Significant
The bare soil						
1	Regression	15069.325	1	15069.325	531.951	0.000[b]
	Residual	1218.122	43	28.328		
	Total	16287.447	44			
Concentrated-lighting Agrivoltaic System						
1	Regression	9917.708	1	9917.708	586.006	0.000[b]
	Residual	727.742	43	16.924		
	Total	10645.451	44			
Even-lighting Agrivoltaic System						
1	Regression	7979.882	1	7979.882	626.057	0.000[b]
	Residual	548.089	43	12.746		
	Total	8527.971	44			

a. Dependent Variable: Cumulative soil surface evaporation (mm) and b. Predictors: (Constant), Evaporation time (d).

3. Results and discussion

3.1. The mechanism of water evaporation reduction under agrivoltaic systems development

Due to surface evaporation, capillary force moves water from the soil profile to the surface. Consequently, water from the soil surface evaporates to form water vapor and diffuses into the atmosphere. Evaporation occurs when water vapor diffuses into the air at the air–water interface. Therefore, reducing the air–water interface interaction can reduce evaporation.

The evaporation restriction mechanism under agrivoltaic systems development is as follows: Firstly, the CAS uses optical interference multilayer films to match the transmittance spectrum and reflection spectrum wavelengths. Thus, the red, blue, and far-red light can be selected and transmitted from sunlight for plants' photosynthesis, and all other wavelengths can be reflected to generate electricity. This means bent glass cover with the multilayer films removes the high-intensity sunlight that impacts the surfaces of water, soil, and plants/crops on the agricultural land and transmits only the intensity impact plants growth (Li et al 2021b, Li et al 2021c). Thus, it can solve the factors influencing water loss, drought, and desertification. **Secondly,** the EAS uses grooves glass in the middle of two PV panels. The grooved glass structure allows sunlight evenly distributed under the grooved glass and PV panels. Therefore, only a part of full sunlight reaches the

Table 4
The output of the SPSS shows a Coefficients[a] table of the three treatments.

Model		Unstandardized Coefficients		Standardized Coefficients	t	Significant
		B	Standard Error	Beta		
The bare soil						
1	(Constant)	23.392	1.614		14.496	0.000
	Evaporation time (d)	1.409	0.061	0.962	23.064	0.000
Concentrated-lighting Agrivoltaic System						
1	(Constant)	17.138	1.247		13.740	0.000
	Evaporation time (d)	1.143	0.047	0.965	24.208	0.000
Even-lighting Agrivoltaic System						
1	(Constant)	12.809	1.082		11.834	0.000
	Evaporation time (d)	1.025	0.041	0.967	25.021	0.000

a. Dependent Variable: Cumulative soil surface evaporation (mm).

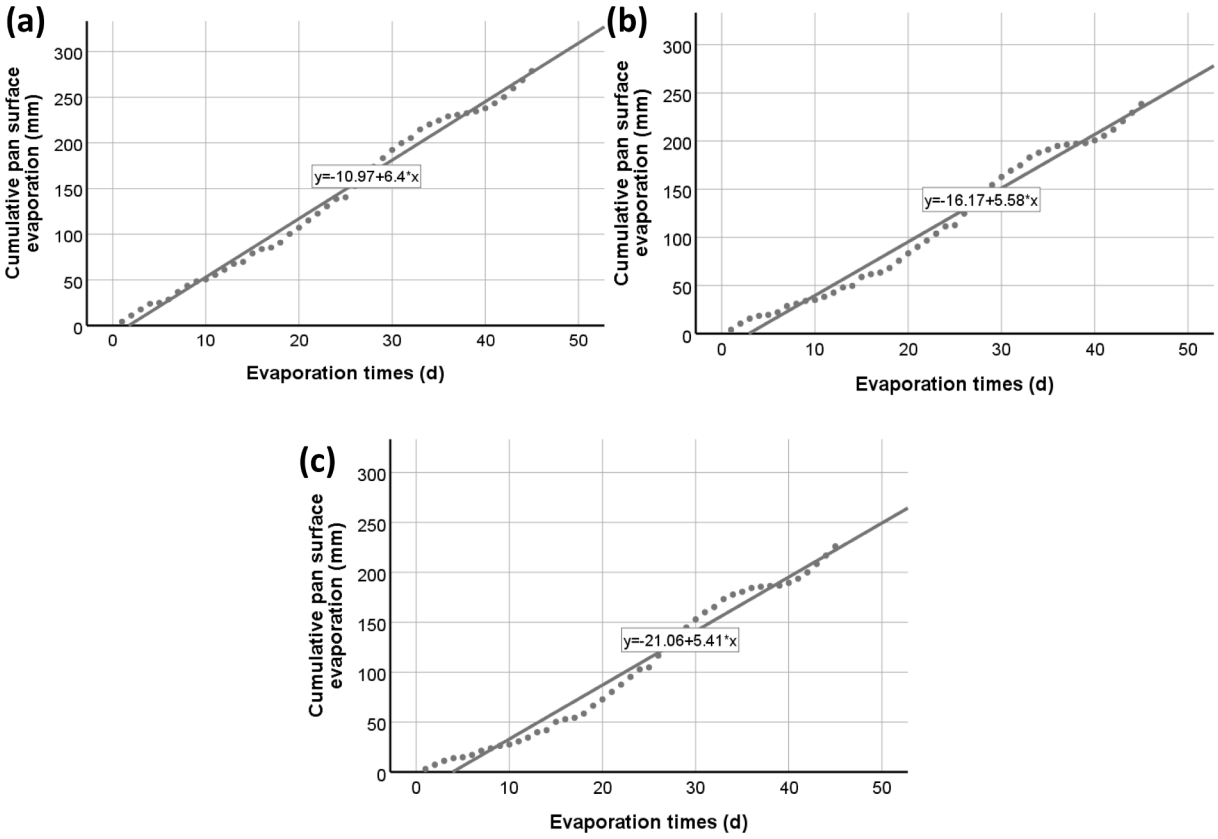

Fig. 7. Cumulative pan surface evaporation and time under three treatments basis on the fitting equation (a) bare soil, (b) under Concentrated-lighting Agrivoltaic System, and (c) Even-lighting Agrivoltaic System.

Table 5
The output of the SPSS shows the model Summary[b] of the three treatments.

Mode	R	R^2	Adjusted R^2	Standard Error of the Estimate
The bare soil				
1	0.996[a]	0.991	0.991	8.06559
Concentrated-lighting Agrivoltaic System				
1	0.991[a]	0.982	0.982	9.92348
Even-lighting Agrivoltaic System				
1	0.989[a]	0.978	0.978	10.71225

a. Predictors: (Constant), Evaporation time (d), and b. Dependent Variable: Cumulative soil surface evaporation (mm).

soil surface under the EAS. Sunlight that reaches the soil's surface can reduce the influence on water loss and land desertification. Therefore, the frequent drought waves and the higher sunlight intensity can be reduced (Zheng et al 2021, Zheng et al 2019). **Thirdly,** the CAS and EAS prevent direct sunlight from reaching the soil surface, thus reducing interaction at the air–water interface. As a result, the processes of the capillary force can be reduced, preventing liquid water from rapidly diffusing off the soil surface. **Finally,** the moisture or vapor contained within the soil surface is relatively high under the CAS and EAS due to poor vapor diffusion. Therefore, water evaporation from the soil and pan surfaces can be reduced.

3.2. *Cumulative evaporation of water from the soil surface:*

As time functions, the cumulative soil surface evaporation processes in all three treatments are shown in Fig. 4b. S1 offers the daily soil surface evaporation analysis. The cumulative soil surface evaporation in the CK, under CAS, and EAS were 80.53 mm, 63.38 mm, and 54.14 mm, respectively. Throughout the 45 days, the control treatment CK had the highest cumulative evaporation; in contrast, the CAS and the EAS had

Table 6
The output of the SPSS shows the analysis variance (ANOVA[a]) of the three treatments.

Mode		Sum of Squares	df	Mean Square	F	Significant
The bare soil						
1	Regression	311340.197	1	311340.197	4785.890	0.000[b]
	Residual	2797.312	43	65.054		
	Total	314137.510	44			
Concentrated-lighting Agrivoltaic System						
1	Regression	236130.016	1	236130.016	2397.858	0.000[b]
	Residual	4234.443	43	98.475		
	Total	240364.459	44			
Even-lighting Agrivoltaic System						
1	Regression	221991.694	1	221991.694	1934.531	0.000[b]
	Residual	4934.346	43	114.752		
	Total	226926.040	44			

a. Dependent Variable: Cumulative soil surface evaporation (mm) and b. Predictors: (Constant), Evaporation time (d).

the lowest cumulative evaporation. Compared with CK, the CAS and EAS have significantly reduced cumulative soil surface evaporation by 21 % and 33 %. The water evaporation from the soil surface is influenced by soil water content and weather conditions. S4 shows the weather conditions recorded during experiment time. This experiment directly exposed the weather conditions on the CK soil surface. Fig. 4a and 4c show the daily soil water evaporation and gradual loss of soil water content (demonstrated in S3). As can be seen quantitatively, the evaporation was significant in the CK in the first eight days, but it was mean in the CAS and EAS. The evaporation was unstable from the ninth to the twenty-eighth day. From the twenty-ninth day until the last day, the evaporation was stable in the CAS and EAS but unstable in the CK. That proves the CAS and EAS can maintain the soil moisture, even if the sunlight intensity is high.

Fig. 4d shows the three treatments' mean temperature during the experiment period. There is a relationship between temperature and intensity of sunlight; when the temperature increases, the sun's intensity also increases. We note that when sunlight is high, the process of water evaporation increases in the CK. In contrast, the sun's intensity under CAS and EAS is low; therefore, evaporation is slow. Consequently, the water evaporation can be reduced. We can notice from Fig. 4d average temperature under the EAS is smaller than that of the CAS, and from Fig. 6C, the intensity of sunlight under the EAS is less than that of CAS. Therefore, the average air temperatures will be highly saturated, which leads to a decrease in the water vapor diffuses to air at the air–water interface at the soil surface under the EAS. Therefore, the accumulation of water evaporation in EAS is less than that of CAS, as shown in Fig. 4a.

In CAS and EAS, soil water content does not influence the evaporation process. However, the soil water content in the CK influenced the evaporation process over the first six days. The soil water evaporation was fast, and the soil water content dropped rapidly. After evaporation, the rapid loss of soil water in the first few days resulted indeed in a soil water shortage. The reach of partial sunlight under the CAS and EAS limited the soil water evaporation to optimize the soil surface under CAS and EAS from the first day to the last day. By the end of the experiments, the soil moisture conservation in CAS and EAS was 35 % and 39 %, respectively, compared to CK at 26 %. Thus, the CAS and EAS saved 33 % and 51 % soil water content.

The SPSS statistical analysis outputs in Fig. 5 and Tables 2, 3, and 4 explain the relationship between evaporation time and cumulative soil surface evaporation in the CK and under CAS and EAS. The coefficients in these tables are the most crucial. They contain the coefficients for the regression equation and tests of significance. The 'B' column in the coefficients (Table 4) in CK, under CAS, and EAS, respectively, gives us the regression line's gradient values and intercept terms. The simple linear regression equation is shown in Fig. 5 for the three treatments. The critical information from Table 2 is the R^2 values of 0.925, 0.932, and 0.936 in CK, under CAS, and EAS, respectively. That indicates only models can explain 92.5 %, 93.2 %, and 93.6 % of the cumulative soil surface evaporation. That is relatively high, so predictions from the regression equation are quite reliable. It also means that the variation of only 7.5 %, 6.8 %, and 6.4 % in CK, under CAS, and EAS, respectively, still need to be investigated further.

Simple linear regression was carried out to investigate the relationship between evaporation time and cumulative soil surface evaporation. The scatterplot showed a strong positive linear relationship between the evaporation time and cumulative evaporation, confirmed by a correlation coefficient shown in Table 2 of 0.962, 0.965, and 0.967 in CK, under CAS, and EAS. Simple linear regression showed a significant relationship between evaporation time and cumulative soil surface evaporation (Significant $= 0.000 < \alpha = 0.05$) shown in the ANOVA Table 3 in CK, under CAS, and EAS. The slope coefficient for the 'B' column in Table 4 were 1.409, 1.143, and 1.025 in KC, under GS, and GMF. Hence, the cumulative soil surface evaporation (mm) increases by 1.409, 1.143, and 1.025 in CK, under CAS and EAS.

3.3. Cumulative evaporation of pan surface evaporation

The cumulative evaporation processes of the pan surface as a function of time are shown in Fig. 6b. The S2 offers the daily water pan evaporation analysis. The cumulative water evaporation of the pan surface in the CK, under the CAS, and the EAS were 278.76 mm, 238.52 mm, and 225.85 mm, respectively. Solar radiation influenced the evaporation process. The reach of partial sunlight on the soil surface under CAS and the EAS impact reduces water evaporation. Fig. 6a is shown the daily soil water evaporation, and Fig. 6a and 6c demonstrate that the evaporation from the pan surface is related to the sun's influence on three treatments. The evaporation was higher on the CK and lowered under the CAS and EAS. That means the total sunlight affects more than partial sunlight on water evaporation. Thus, under CAS and EAS, the amount of sun reaching soil and pan surfaces is less than that of the CK. Compared to CK, the cumulative water surface evaporation

Table 7
The output of the SPSS shows a Coefficients[a] table of the three treatments.

Model		Unstandardized Coefficients		Standardized Coefficients	t	Significant
		B	Standard Error	Beta		
The bare soil						
1	(Constant)	−10.969	2.445		−4.486	0.000
	Evaporation time (d)	6.405	0.093	0.996	69.180	0.000
Concentrated-lighting Agrivoltaic System						
1	(Constant)	−16.172	3.009		−5.375	0.000
	Evaporation time (d)	5.578	0.114	0.991	48.968	0.000
Even-lighting Agrivoltaic System						
1	(Constant)	−21.060	3.248		−6.484	0.000
	Evaporation time (d)	5.408	0.123	0.989	43.983	0.000

a. Dependent Variable: Cumulative soil surface evaporation (mm).

under CAS and EAS was decreased by 14 % and 19 %. Thus, the cumulative pan surface evaporation value under the CAS and EAS reduces water evaporation significantly.

That proves the CAS and EAS allow the soil surface to be reached only spectrum wavelengths that provide plants with photosynthesis—blocking several unnecessary sunlight wavelengths. For 45 days, the average solar radiation under EAS and CAS was 22 %, and 28 compared to CK was 55 %. The previous findings support the conclusions of these investigations, showing that under the influence of CAS, evaporation can be reduced by more than 25 %. This evaporation reduction significantly impacts crop quality and yield (Li et al 2021c, Liu et al 2018).

The SPSS statistical analysis outputs in Fig. 7 and Tables 5, 6, and 7 explain the relationship between evaporation time and cumulative pan surface evaporation in the CK, under CAS, and EAS. The coefficients in the table are the most crucial ones. The coefficients for the regression equation and the evaluation for significance are shown in Table 5. The 'B' column in Table 7 in KC, under CAS, and EAS, gives the values of the gradient and interception terms for the regression line. The simple linear regression equation is shown in Fig. 7. The critical information from Table 5 is the R^2 values of 0.991, 0.982, and 0.978 in CK, under CAS, and EAS, indicating that only models can explain 99.1 %, 98.2 %, and 97.8 % cumulative pan surface evaporation. That is relatively high, so predictions from the regression equation are reasonably trustable. It also means that only 0.9 %, 1.8 %, and 2.2 % in CK, under CAS, and EAS, of the variation, is still unexplained; thus, adding other independent variables could improve the fit of the models.

The relationship between evaporation time and cumulative surface evaporation was investigated using simple linear regression. Based on the scatterplot, we found a strong positive linear relationship between evaporation time and cumulative evaporation, as shown in Table 5. We obtained correlation coefficients of 0.996, 0.991, and 0.989 for the CK, CAS, and EAS variables. Simple linear regression showed a significant relationship between evaporation time and cumulative pan surface evaporation (Significant $= 0.000 < \alpha = 0.05$) shown in the ANOVA Table 6 in KC, under CAS and EAS. The slope coefficient in the 'B' column in Table 7 was 6.405, 6.578, and 5.408 in CK, respectively, under CAS and EAS. Hence, the cumulative soil surface evaporation increases by 6.405, 6.578, and 5.408 in CK under CAS and EAS.

4. Conclusion:

The agrivoltaic systems have grown worldwide in recent years. The major advantages are to generate electricity and crop growth simultaneously on the same land. This paper presents strong evidence from a quantitative study of reduced water evaporation, which is the third benefit of the AgriVoltaic Systems Development (AVSD). Our study results have shown that sunlight can pass through AVSD to reach the ground, and water evaporation reduction occurs significantly. We determined CK's cumulative soil and pan surface evaporation under CAS and EAS. We investigated the relationship between cumulative surface evaporation and evaporation time using SPSS software. Our results are summarized below:

a. The cumulative soil surface evaporation during the experiment period in the CK, under the CAS, and the EAS were 80.53 mm, 63.38 mm, and 54.14 mm; thus, CAS and EAS significantly reduced water evaporation at 21 % and 33 % of the soil surface evaporation.
b. The cumulative evaporation of the pan surface during the experiment period in the CK, under the CAS, and the EAS were 278.76 mm, 238.52 mm, and 225.85 mm; thus, the CAS and EAS significantly reduced water evaporation at 14 % and 19 % of the pan surface evaporation.
c. By the end of the experiment, the soil water content during the experiment period of CK, CAS, and EAS was considered a total of 26 %, 35 %, and 39 %, respectively. Thus, the CAS and EAS have saved soil water content at 33 % and 51 %.
d. According to the data logged by meteorological stations for three experimental treatments, the average solar radiation of the total time of the experiment (45 days) in the CK, under the CAS, and the EAS was 55 %, 28 %, and 22 %.

We trust that the AVSD could help overcome the challenges of water scarcity, food supply, and energy production simultaneously on the same land.

Declaration of Competing Interest

The authors declare that they have no known competing financial interests or personal relationships that could have appeared to influence the work reported in this paper.

Acknowledgements

This work was supported by "Fuyang Municipal Government - Fuyang Normal University Horizontal Project" under grant SXHZ202011 and "the CRSRI Open Research Program" under grant CKWV2019726/KY, and "the Fundamental Research Funds for the Central Universities" under grant WK529000000, Anhui Provincial Science and Technology Major Project" under grant No: 202203a06020002.

Appendix A. Supplementary data

Supplementary data to this article can be found online at https://doi.org/10.1016/j.solener.2022.10.022.

References

AbdAllah, A., 2019. Impacts of Kaolin and Pinoline foliar application on growth, yield and water use efficiency of tomato (Solanum lycopersicum L.) grown under water deficit: A comparative study. Journal of the Saudi Society of Agricultural Sciences 18, 256–268.

AbdAllah, A.M., Mashaheet, A.M., Zobel, R., Burkey, K.O., 2019. Physiological basis for controlling water consumption by two snap beans genotypes using different anti-transpirants. Agric. Water Manag. 214, 17–27.

Abdallah, A.M., Parihar, C.M., Patra, S., Nayak, H.S., Saharawat, Y.S., et al., 2021. Critical evaluation of functional aspects of evaporation barriers through environmental and economics lens for evaporation suppression - A review on milestones from improved technologies. Sci. Total Environ. 788, 147800.

Adams, J.E., 1966. Influence of Mulches on Runoff, Erosion, and Soil Moisture Depletion. Soil Sci. Soc. Am. J. 30, 110–114.

Ali Abaker Omer, A., Li, M., Liu, W., Liu, X., Zheng, J., et al., 2022. Water Evaporation Reduction Using Sunlight Splitting Technology. Agronomy 12, 1067.

Allardyce, C.S., Fankhauser, C., Zakeeruddin, S.M., Grätzel, M., Dyson, P.J., 2017. The influence of greenhouse-integrated photovoltaics on crop production. Sol. Energy 155, 517–522.

Alvarez, V.M., Baille, A., Martínez, J.M.M., González-Real, M.M., 2006. Efficiency of shading materials in reducing evaporation from free water surfaces. Agric. Water Manag. 84, 229–239.

Andrews, J.H., Crescimanno, M., Dawson, N.J., Mao, G., Petrus, J.B., et al., 2012. Folding flexible co-extruded all-polymer multilayer distributed feedback films to control lasing. Opt. Express 20, 15580–21558.

Awan, K.S., 2009. Effect of Mulch on Soil Physical Properties and N, P, K Concentration in Maize (Zea mays) Shoots under Two Tillage Systems. International Journal of Agriculture & Biology 11, 119–124.

Awodoyin, R., Ogbeide, F., Oluwole, O., 2010. Effects of three mulch types on the growth and yield of tomato (Lycopersicon esculentum Mill.) and weed suppression in Ibadan, rainforest-savanna transition zone of Nigeria. Tropical Agricultural Research and Extension 10.

Barron-Gafford, G.A., Pavao-Zuckerman, M.A., Minor, R.L., Sutter, L.F., Barnett-Moreno, I., et al., 2019. Agrivoltaics provide mutual benefits across the food–energy–water nexus in drylands. Nat. Sustainability 2, 848–855.

By Jim Bilskie PD. Soil water status: content and potential. *Campbell Scientific, Inc* 435 Condon LE, Atchley AL, Maxwell RM. 2020. Evapotranspiration depletes groundwater under warming over the contiguous United States. *Nature Communications* 11: 873.

Cossu, M., Murgia, L., Ledda, L., Deligios, P.A., Sirigu, A., et al., 2014. Solar radiation distribution inside a greenhouse with south-oriented photovoltaic roofs and effects on crop productivity. Appl. Energy 133, 89–100.

Elamri, Y., Cheviron, B., Lopez, J.M., Dejean, C., Belaud, G., 2018. Water budget and crop modelling for agrivoltaic systems: Application to irrigated lettuces. Agric. Water Manag. 208, 440–453.
El-Ghannam, M.K., Aiad, M.A., Abdallah, A.M., 2021. Irrigation efficiency, drain outflow and yield responses to drain depth in the Nile delta clay soil. Egypt. *Agricultural Water Management* 246, 106674.
Goetzberger, A., Zastrow, A., 1982. On the Coexistence of Solar-Energy Conversion and Plant Cultivation. International Journal of Solar Energy 1, 55–69.
Gorjian, S., Bousi, E., Özdemir, Ö.E., Trommsdorff, M., Kumar, N.M., et al., 2022. Progress and challenges of crop production and electricity generation in agrivoltaic systems using semi-transparent photovoltaic technology. Renew. Sustain. Energy Rev. 158, 112126.
Greve, P., Kahil, T., Mochizuki, J., Schinko, T., Satoh, Y., et al., 2018. Global assessment of water challenges under uncertainty in water scarcity projections. Nat. Sustainability 1, 486–494.
Hassanien, R.H.E., Li, M., Yin, F., 2018. The integration of semi-transparent photovoltaics on greenhouse roof for energy and plant production. Renewable Energy 121, 377–388.
Hassanpour Adeh, E., Selker, J.S., Higgins, C.W., 2018. Remarkable agrivoltaic influence on soil moisture, micrometeorology and water-use efficiency. PLoS ONE 13, e0203256.
Homma, M., Doi, T., Yoshida, Y., 2016. A field experiment and the simulation on agrivoltaic-systems regarding to rice in a paddy field. J Jpn Soc Energy Resour 37, 23-31.
Hunt, J.R., Celestina, C., Kirkegaard, J.A., 2020. The realities of climate change, conservation agriculture and soil carbon sequestration. Glob. Change Biol. 26, 3188–3319.
Hwang, H., An, S., Lee, B., Chun, C., 2020. Improvement of Growth and Morphology of Vegetable Seedlings with Supplemental Far-Red Enriched LED Lights in a Plant Factory. Horticulturae 6, 109.
Jones, G.F., Evans, M.E., Shapiro, F.R., 2022. Reconsidering beam and diffuse solar fractions for agrivoltaics. Sol. Energy 237, 135–143.
Kasahara, M., Kagawa, T., Sato, Y., Kiyosue, T., Wada, M., 2004. Phototropins Mediate Blue and Red Light-Induced Chloroplast Movements in Physcomitrella patens. Plant Physiol. 135, 1388–1397.
Kasirajan, S., Ngouajio, M., 2012. Polyethylene and biodegradable mulches for agricultural applications: a review. Agron. Sustainable Dev. 32, 501–529.
Khorsandi, F., 2011. Soil Water Conservation by Course Textured Volcanic Rock Mulch. Society of Applied Sciences 2 (4).
Knowles, J.F., Blanken, P.D., Williams, M.W., Chowanski, K.M., 2012. Energy and surface moisture seasonally limit evaporation and sublimation from snow-free alpine tundra. Agric. For. Meteorol. 157, 106–115.
Kumar, M., Haillot, D., Gibout, S., 2022. Survey and evaluation of solar technologies for agricultural greenhouse application. Sol. Energy 232, 18–34.
Lemon, E.R., 1956. The Potentialities for Decreasing Soil Moisture Evaporation Loss. Soil Sci. Soc. Am. J. 20, 120–215.
Li, M., Liu, W., Zhang, F., Zhang, X., Abaker Omer, A.A., et al., 2021b. Polymer multilayer film with excellent UV-resistance & high transmittance and its application for glass-free photovoltaic modules. Sol. Energy Mater. Sol. Cells 229, 111103.
Li, M., Liu, Y., Zhang, F., Zhang, X., Zhang, Z., et al., 2021c. Design of multi-passband polymer multilayer film and its application in photovoltaic agriculture. Chinese Optics Letters 19, 112201.
Li, C.-L., Shi, K.-B., Yan, X.-J., Jiang, C.-L., 2021a. Experimental Analysis of Water Evaporation Inhibition of Plain Reservoirs in Inland Arid Area with Light Floating Balls and Floating Plates in Xinjiang. China. *Journal of Hydrologic Engineering* 26, 04020060.
Liao, Y., Cao, H.-X., Liu, X., Li, H.-T., Hu, Q.-Y., Xue, W.-K., 2021. By increasing infiltration and reducing evaporation, mulching can improve the soil water environment and apple yield of orchards in semiarid areas. Agric. Water Manag. 253, 106936.
Liu LQ, Guan CG, Zhang FX, Li M, Lv H, et al. 2017. A Novel Application for Concentrator Photovoltaic in the Field of Agriculture Photovoltaics. *Aip Conf Proc* 1881.
Liu, H.-J., Kang, Y., 2007. Sprinkler irrigation scheduling of winter wheat in the North China Plain using a 20 cm standard pan. Irrig. Sci. 25, 149–159.
Liu, W., Liu, L., Guan, C., Zhang, F., Li, M., et al., 2018. A novel agricultural photovoltaic system based on solar spectrum separation. Sol. Energy 162, 84–94.
Loftus SC. 2022. Chapter 19 - Simple linear regression In *Basic Statistics with R*, ed. SC Loftus, pp. 227-47: Academic Press.
Loz B. November 17, 2020. What Are The Disadvantages of Mulching? *https://takeayard.com/mulching-disadvantages/*.
Lu, L., Effendy Ya'acob, M., Shamsul Anuar, M., Nazim, M.M., 2022. Comprehensive review on the application of inorganic and organic photovoltaics as greenhouse shading materials. Sustainable Energy Technol. Assess. 52, 102077.
Marrou, H., Wery, J., Dufour, L., Dupraz, C., 2013. Productivity and radiation use efficiency of lettuces grown in the partial shade of photovoltaic panels. Eur. J. Agron. 44, 54–66.
McKuin, B., Zumkehr, A., Ta, J., Bales, R., Viers, J.H., et al., 2021. Energy and water co-benefits from covering canals with solar panels. Nat. Sustainability 4, 609–617.
Meziani, A., Remini, B., Boutoutaou, D., 2020. Estimating evaporation from dam-reservoirs in arid and semi arid regions case of Algeria. J. Eng. Appl. Sci. 15, 2097–2107.
Morsy, S.M., Elbasyoni, I.S., Abdallah, A.M., Baenziger, P.S., 2021. Imposing water deficit on modern and wild wheat collections to identify drought-resilient genotypes. J. Agron. Crop Sci.
Mueller, B., Hirschi, M., Jimenez, C., Ciais, P., Dirmeyer, P.A., et al., 2013. Benchmark products for land evapotranspiration: LandFlux-EVAL multi-data set synthesis. Hydrol. Earth Syst. Sci. 17, 3707–3720.
Neupane Bhandari, S., Schlüter, S., Kuckshinrichs, W., Schlör, H., Adamou, R., Bhandari, R., 2021. Economic Feasibility of Agrivoltaic Systems in Food-Energy Nexus Context: Modelling and a Case Study in Niger. Agronomy 11, 1906.
Nguyen, T.B.T., Nguyen, T.H.N., Pham, Q.T., 2020. Water loss due to evaporation from open reservoirs under weather conditions in Vietnam. Asia-Pac. J. Chem. Eng. 15, e2488.
Nyamoti M. 16/6/2020. State four disadvantages of organic mulches. *https://www.atikaschool.org/agriculturetopicalquestions/state-four-disadvantages-of-organic-mulches*.
Obergfell T, Schnidele S, Bopp G, Goetzberger A, Reise C. *Energy Economics of Phasing out Carbon and Uranium, 13th IAEE European Conference, August 18-21, 20132013*. International Association for Energy Economics.
2. OECD environmental outlook to 2050: the consequences of inaction. *International Journal of Sustainability in Higher Education* 13.
Riaz, M.H., Imran, H., Younas, R., Butt, N.Z., 2021. The optimization of vertical bifacial photovoltaic farms for efficient agrivoltaic systems. Sol. Energy 230, 1004–1012.
Schindele, S., Trommsdorff, M., Schlaak, A., Obergfell, T., Bopp, G., et al., 2020. Implementation of agrophotovoltaics: Techno-economic analysis of the price-performance ratio and its policy implications. Appl. Energy 265, 114737.
Shalaby, M.M., Nassar, I.N., Abdallah, A.M., 2021. Evaporation suppression from open water surface using various floating covers with consideration of water ecology. J. Hydrol. 598, 126482.
Singer, K.D., Kazmierczak, T., Lott, J., Song, H., Wu, Y., et al., 2008. Melt-processed all-polymer distributed Bragg reflector laser. Opt. Express 16, 10358–10363.
Sonneveld, P.J., Swinkels, G.L.A.M., Bot, G.P.A., Flamand, G., 2010a. Feasibility study for combining cooling and high grade energy production in a solar greenhouse. Biosyst. Eng. 105, 51–58.
Sonneveld, P.J., Swinkels, G.L.A.M., Campen, J., van Tuijl, B.A.J., Janssen, H.J.J., Bot, G. P.A., 2010b. Performance results of a solar greenhouse combining electrical and thermal energy production. Biosyst. Eng. 106, 48–57.
Tesfuhuney, W.A., Van Rensburg, L.D., Walker, S., Allemann, J., 2015. Quantifying and predicting soil water evaporation as influenced by runoff strip lengths and mulch cover. Agric. Water Manag. 152, 7–16.
Valle, B., Simonneau, T., Sourd, F., Pechier, P., Hamard, P., et al., 2017. Increasing the total productivity of a land by combining mobile photovoltaic panels and food crops. Appl. Energy 206, 1495–1507.
Waheeb Youssef, Y., Khodzinskaya, A., 2019. A Review of Evaporation Reduction Methods from Water Surfaces. E3S Web Conf. 97, 05044.
Weber, M.F., Stover, C.A., Gilbert, L.R., Nevitt, T.J., Ouderkirk, A.J., 2000. Giant Birefringent Optics in Multilayer Polymer Mirrors. Science 287, 2451–3246.
Weselek, A., Bauerle, A., Zikeli, S., Lewandowski, I., Högy, P., 2021. Effects on Crop Development, Yields and Chemical Composition of Celeriac (Apium graveolens L. var. rapaceum) Cultivated Underneath an Agrivoltaic System. *Agronomy* 11, 733.
Wu, Y., Du, T., Ding, R., Yuan, Y., Li, S., Tong, L., 2017. An isotope method to quantify soil evaporation and evaluate water vapor movement under plastic film mulch. Agric. Water Manag. 184, 59–66.
Xie, Z., Wang, Y., Jiang, W., Wei, X., 2006. Evaporation and evapotranspiration in a watermelon field mulched with gravel of different sizes in northwest China. Agric. Water Manag. 81, 173–184.
Xue, J., 2017. Photovoltaic agriculture - New opportunity for photovoltaic applications in China. Renew. Sustain. Energy Rev. 73, 1–9.
Yano, A., Furue, A., Kadowaki, M., Tanaka, T., Hiraki, E., et al., 2009. Electrical energy generated by photovoltaic modules mounted inside the roof of a north–south oriented greenhouse. Biosyst. Eng. 103, 228–238.
Yano, A., Kadowaki, M., Furue, A., Tamaki, N., Tanaka, T., et al., 2010. Shading and electrical features of a photovoltaic array mounted inside the roof of an east–west oriented greenhouse. Biosyst. Eng. 106, 367–377.
Yuan, C., Lei, T., Mao, L., Liu, H., Wu, Y., 2009. Soil surface evaporation processes under mulches of different sized gravel. Catena 78, 117–121.
Zhang, Z., Zhang, F., Li, M., Liu, L., Lv, H., et al., 2018. Progress in agriculture photovoltaic leveraging CPV. AIP Conf. Proc. 2012, 110006.
Zhao, G., Gao, H., 2019. Estimating reservoir evaporation losses for the United States: Fusing remote sensing and modeling approaches. Remote Sens. Environ. 226, 109–124.
Zheng, J., Zhang, X., Ning, X., Ingenhoff, J., Liu, W., 2019. An improved photovoltaic agriculture system with groove glass plate. SPIE, p. pp. PA..
Zheng, J., Meng, S., Zhang, X., Zhao, H., Ning, X., et al., 2021. Increasing the comprehensive economic benefits of farmland with Even-lighting Agrivoltaic Systems. PLoS ONE 16, e0254482.
Zribi, W., Aragüés, R., Medina, E., Faci, J.M., 2015. Efficiency of inorganic and organic mulching materials for soil evaporation control. Soil Tillage Res. 148, 40–45.